Tetrahedron 73 (2017) 4979–4987

Contents lists available at ScienceDirect

Tetrahedron

journal homepage: www.elsevier.com/locate/tet

Native protein hydrogels by dynamic boronic acid chemistry

Christiane Seidler [a, b], David Y.W. Ng [a, **], Tanja Weil [a, b, *]

[a] Max Planck Institute for Polymer Research, Ackermannweg 10, 55128 Mainz, Germany
[b] Ulm University, Albert-Einstein-Allee 11, 89081 Ulm, Germany

ARTICLE INFO

Article history:
Received 18 May 2017
Received in revised form
27 June 2017
Accepted 28 June 2017
Available online 29 June 2017

Keywords:
Dynamic covalent chemistry
Stimulus responsive
Cytochrome C
Boronic acid
Hydrogel

ABSTRACT

Bioactive protein-based materials are unique functional systems that incorporate the specificity and intelligent characteristics of biomolecules within synthetic polymers. Herein, we take advantage of the boronic acid/salicyl hydroxamate molecular recognition strategy to crosslink an apoptosis inducing enzyme, cytochrome c, by dynamic covalent interactions to form a bioactive and responsive hydrogel for controlled administration. The material exhibits attractive rheological properties with high storage modulus and modulus crossover despite the perceived conformational sensitivity of the proteins. Upon acidification, the hydrogel matrix dissociated and release active enzymes into A549 cells, which initiates apoptosis. In combination, the chemical strategy facilitates the integration of native enzymes structurally into the hydrogel scaffold while simultaneously providing biological activity under a stimulus controlled release mechanism.

1. Introduction

The evolution of chemistry – from static to dynamic, where molecular bonds or supramolecular interactions are able to reorganize and exchange in a programmable fashion, has been realized as a fundamental feature in creating intelligent materials on multiple length-scales.[1–3] This strategy has been used by Nature and refined to near-perfection which we now bear witness to its many creations. In all these biologically complex systems, both dynamic covalent chemistry and supramolecular chemistry play a central role in all networks and processes from the transport of small molecules to hierarchical superstructures of macromolecular assemblies.[4,5]

Supramolecular chemistry provides intrinsic and geometric variations based on hydrogen, ionic bonds and π-π networks, whereas dynamic covalent chemistry is to a large extend found in disulfide bridges of proteins and peptides. Although deceptively simple in terms of chemistry, disulfide bonds dictate bioactivities that require a change in protein conformation/folding as well as in defining the energy landscapes of many structures.[6] Hence, disulfide bridges are the most conserved (>95%) functionality across the proteome.[7] The importance of this functional moiety is further emphasized by protein disulfide isomerase, a molecular chaperone that bridges cysteine residues in proteins, which accounts for up to 0.8% of total cellular protein.[8] Based on the number and placements of cysteine residues, mechanical properties of proteins (i.e. keratin, collagen),[6] its functions (i.e. vascular endothelial growth factors, integrin)[9] as well as entire systems (i.e. virus maturation)[10] are engineered within the dynamics of disulfide chemistry.

Specifically, dynamic covalent chemistry is used to create entropically driven folding and allows the existence of multiple stable conformations of proteins for their function. In this way, dynamic covalent structure formation ensures that misfolded peptide sequences are not self-assembled into toxic aggregates.[11] As such, dynamic covalent bonds impart both chemical flexibility and stability in the entire biological system. Similarly, dynamic covalent bonds currently available in synthetic chemistry are rather limited in variety as stimulus responsive groups are typically irreversible in order to drive the reaction forward. Among those that are reversible, the selection narrows further if compatibility towards the physiological conditions is required. Herein, we select a strategy based on boronic acids that is i.e. non-toxic, biorthogonal, rapid, stable and therefore fulfils the stringent

* Corresponding author. Max Planck Institute for Polymer Research, Ackermannweg 10, 55128 Mainz, Germany.
** Corresponding author. Max Planck Institute for Polymer Research, Ackermannweg 10, 55128 Mainz, Germany.
E-mail address: weil@mpip-mainz.mpg.de (T. Weil).

http://dx.doi.org/10.1016/j.tet.2017.06.066

demands as responsive chemical functionality for biomedical applications.[12]

Boronic acids form stable and reversible complexes with *cis*-diols in a pH-dependent manner under aqueous conditions.[13] The stability of these boronic esters relies on 1) the steric bulk of the diol to resist hydrolysis, 2) electron orbital overlap thus favouring O-donors compared to N-donors, 3) molecular geometry to fit the small boron center.[14] Hence, several systems of boronic acid interactions have been reported including the complexation with various carbohydrates, catechol derivatives as well as salicyl hydroxamates.[15] Among these substrates, salicyl hydroxamates represent the highest binding affinity and their use with boronic acids ranges from a click-like ligation of peptides[16] to the construction of pH-responsive macromolecular systems.[17,18] Extending the application repertoire of the reaction, we investigate the use of this dynamic complexation in building native protein hydrogel systems.

In general, hydrogels are typically made from covalently cross-linked or supramolecular polymers. Based on the type of intramolecular linkage, the mechanical properties can be customized. Recently, proteins have received increasing attention as scaffold materials[19] and/or crosslinkers[20,21] to form biocompatible and responsive materials. However, the use of therapeutically relevant enzymes within the gel matrix was not reported before. Enzymes are catalytic proteins that are extremely sensitive and most chemical techniques often cause denaturation of the protein. The advantage of using enzymes as a matrix component means that the exact stoichiometry is precise compared to a typical encapsulation procedure where the enzyme is trapped within a cross-linked polymer. Local administration of apoptosis (programmed cell death) inducing proteins in a hydrogel matrix provides great opportunities to control growth of e.g. tumor or bone-degrading cells for therapy.[22]

We report herein the formation of a native protein hydrogel by crosslinking cytochrome c (CytC), an important enzyme that initiates apoptosis, with poly(ethyleneglycol) (PEG) using boronic acid-salicyl hydroxamate (PBA-SHA) chemistry. By incorporating these components, we aim to create a dynamic hydrogel that is biocompatible, enzymatically active, pH-responsive and self-healing. This combination provides a new perspective where sensitive (bio)molecules can now be easily integrated as matrix components in an elegant way.

2. Results and discussion

Both hydrogel components, the CytC protein and PEG, were modified correspondingly with boronic acid and salicyl hydroxamate moieties (Fig. 1, Scheme 1). CytC is a 12.4 kDa protein that contains 20 amino groups in its sequence, allowing modification with 4-carboxyphenylboronic acid succinimidyl ester. The modification of the protein was accomplished efficiently in phosphate buffer (pH 8.0, 50 mM) with an excess of 4-carboxyphenylboronic acid succinimidyl ester (18 eq.). The boronic acid modified CytC (CytC-BA) was purified by ultrafiltration (5 kDa MWCO) and the number of boronic acid residues was found to be 11 (MALDI-TOF MS, Supporting Fig. S1).

In order to cross-link CytC-BA, PEG_{2000} was selected as it is a hygroscopic scaffold that retains water and at the same time extremely flexible to dynamically exchange within the matrix. PEG_{2000}-$(NH_2)_2$ was first transformed into PEG_{2000}-$(N_3)_2$ by an azido transfer reaction. Subsequently, PEG_{2000}-$(N_3)_2$ underwent a copper-catalyzed azide-alkyne cycloaddition using Trt-protected ethynyl salicyl hydroxamic acid and acid deprotection of the intermediate affords the target crosslinker PEG_{2000}-$(SHA)_2$ in good yields. A longer analogue using PEG_{3000} was synthesized to study the effect of chain length and hence the amount of trapped water molecules on the system. In addition, a 4-arm PEG_{2000} was also selected as an investigation towards how multivalent binding events affect rheological properties while keeping the relative number of water molecules constant.

2.1. Hydrogel formation and rheological properties

The hydrogel was first constructed by varying the stoichiometry of the crosslinker (0.5, 1.0, 1.5 mol eq. with respect to each boronic acid/salicyl hydroxamate binding event). With a 8 wt% CytC-BA, a hydrogel was instantaneously formed upon the addition of the cross-linker for all three stoichiometry at pH 7.4. The kinetics of gelation was monitored by a rheometer through the increase of both the storage modulus (G′) and the loss modulus (G″) with incubation time. As a representative example, Fig. 2A shows the steady increase of G′ as well as the G′/G″ ratio as the components gel, implying that the dynamic covalent bonds between the boronic acid and the SHA are formed over time attributing the material its strength and stiffness. Comparing across different stoichiometry of

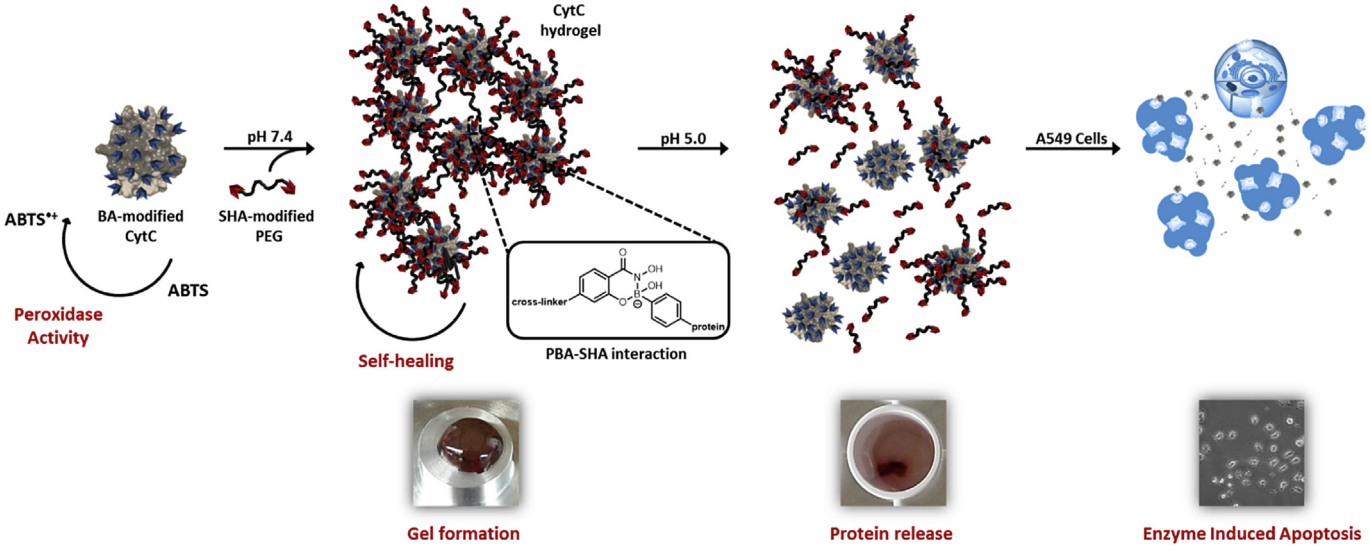

Fig. 1. Schematic of a pH-responsive hydrogel synthesized using cytochrome c as a bioactive protein precursor.

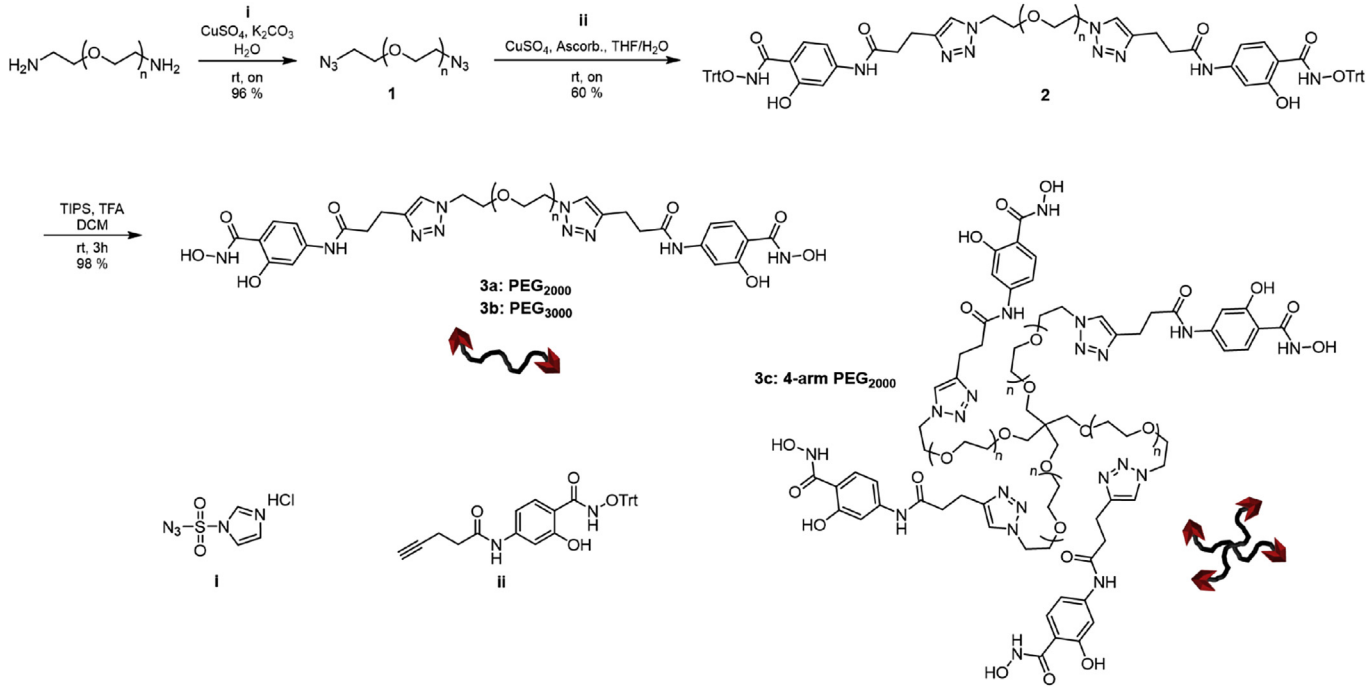

Scheme 1. Synthesis of salicyl hydroxamate functionalized poly(ethyleneglycol) cross linkers.

linear PEG_{2000}-$(SHA)_2$ as the cross-linker (Fig. 2B), the storage modulus showed an expected increase with higher amounts of cross-linker reaching a maximum value of ~56 kPa (1.5 eq **3a**). The strength of the gel can also be raised by increasing the binding units per cross-linker as the 4-arm PEG_{2000}-$(SHA)_4$ demonstrated a higher G′ value (~58 kPa). However, comparing the modulus magnitude alone is insufficient for a material that is designed to have responsive dynamics. Ideally, it should possess a balance between stiffness, elasticity and regeneration.

The materials were subjected to an oscillatory strain up to 1000% in order to test their mechanical stability (Fig. 2C). In this experiment, the oscillatory strain on the hydrogel increased with time until the gel collapses. When the matrix becomes more like an elastic fluid, the value of the loss modulus G″ exceeds the storage modulus G′ and the corresponding amount of strain exerted is defined as the modulus crossover. Interestingly, the hydrogel made with 1.5 mol eq. of PEG_{2000}-$(SHA)_2$ is significantly weaker as the modulus crossover (~190%) is about 2.5 fold lower compared to the hydrogel made with less cross linker amount (Fig. 2D). This observation suggests that the intermolecular forces of the matrix are much weaker because the excess functionalities are constantly exchanging making the internal nanostructures more fluid. In contrast, an equimolar amount of PEG_{2000}-$(SHA)_2$ provides the highest capacity (~440%) for oscillatory stress, which corresponds to the maximum possible interactions between CytC-BA and the cross-linker.

Next, we investigate the effect of multivalent interactions as well as cross-linker length on the mechanical properties. An increase in polymer chain length from PEG_{2000} to PEG_{3000} results in a 2 fold decrease in both storage and loss modulus. This is most likely attributed to the increase in polymer flexibility and water retention in the hydrogel thereby reducing its stiffness. Although the gel appears more fluid, the internal structures remain robust up to 290% oscillatory strain. Comparatively, a 4-arm cross-linker PEG_{2000}-$(SHA)_4$, shared similar mechanical properties with linear PEG_{2000}-$(SHA)_2$ with high stability and stiffness.

Although it is challenging to provide head-to-head comparisons, many hydrogels derived from covalently crosslinked biomaterials such as chitosan,[23] hyaluronic acids,[24] DNA[25] and peptides[26] are often less stiff by an order of magnitude. We hypothesize that the rigid secondary and tertiary structures of the native protein has a multiplicative effect on the storage and loss modulus of the bulk material. In addition, the globular structure of a native protein generally contains less water molecules due to its compact three-dimensional structure compared to linear chains of biopolymers of equivalent molecular weight. Thus, it is reasonable to postulate that the entire system is stiffer as a result of lower water content.

2.2. pH responsiveness

As these gels are formed based on the interactions between the boronic acid and SHA, the properties of the material will likewise be dependent on the integrity of these dynamic covalent bonds. Since, the boronic acid-SHA bonds can be dissociated under aqueous acidic conditions (pH 5.0), we subsequently investigate the pH responsiveness of the constructed hydrogel. Upon acidification to pH 5.0, the hydrogel can be seen optically to dissolve within 2 min with the corresponding release of CytC-BA (Fig. 3A). As CytC is a heme protein that possesses a unique absorbance spectrum, the kinetics of dissolution and release of the protein can be monitored via UV–vis spectroscopy (Fig. 3B). Two controls were implemented in this experiment: 1) a negative and background control at pH 7.4 and 2) a solution of free CytC that was used to construct the hydrogel. The release profile shows that 100% of the protein is steadily released within 22 h. In contrast, <10% of the protein is released at pH 7.4 within the same timeframe due to dilution effects. In addition, rheology measurements were also conducted while the hydrogel is acidified (Fig. 3C). The moduli of the gel matrix were monitored and showed a rapid decrease over time eventually reaching a steady state at 1 h. The residual mechanical strength present in the gel can be attributed to supramolecular

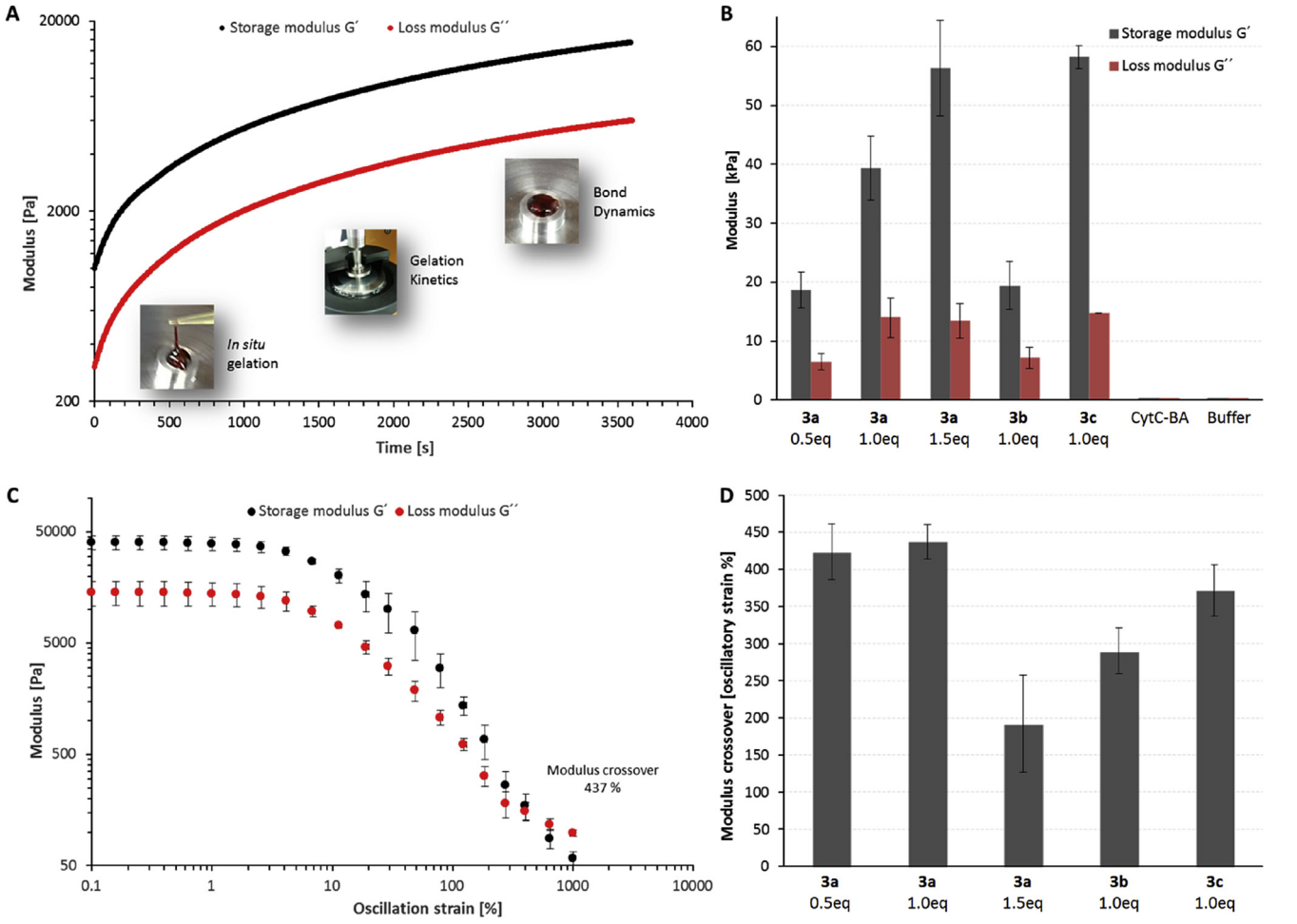

Fig. 2. Rheological studies on CytC-BA hydrogel. A) Gelation kinetics monitored as the increase of storage modulus (G′) and loss modulus (G″) over time. B) Variation of cross-linker stoichiometry, chain length and number of BA-SHA binding motifs and the resultant G′, G″ values at steady state. C) Viscoelasticity change of CytC-BA hydrogel when subjected to increasing oscillatory strain (0.1%–1000%). Modulus crossover is defined as the moment when G″ exceeds G′. D) Summary of modulus crossover points for all analogues of cross-linkers.

interactions between the PEG chains and the protein at high concentrations that are pH independent.

2.3. Self-healing properties

The main highlight of using dynamic covalent bonds is that it essentially creates a highly stiff material while simultaneously providing the capability of self-healing due to dynamic bond exchange. These properties were also similarly observed by Jung's group using hydrazones as crosslinking chemistry between calix[4]arene hydrazide and diphenyl terephthalate derivative ($G' \geq 10$ kPa).[27] In comparison, supramolecular strategies based on host-guest chemistry (i.e. curcubit[7,8]uril),[28,29] or hydrogen bonds[30] have generally lower stiffness ($G' \leq 10$ kPa) and modulus crossover points per interacting motif but reveal often greater self-regeneration properties.

Especially for therapeutic purposes, a self-healing property is important because the release or dissociation kinetics of the material should not be affected by mechanical stress. Preliminary tests were conducted by physically cutting the gel into two and allow the pieces to re-attach. Indeed, the individual components were successfully rejoined within 5 min (Fig. 4A). Further elaborated investigations were accomplished by subjecting the hydrogel to a cyclic oscillatory strain (0.1–1000%) on the rheometer. At 1000% strain, the gel was completely destroyed and was allowed to heal by resetting the oscillatory strain to 0.1%.

For all gels cross-linked with linear PEG, immediate recovery to 40–50% of the original moduli was observed within 5 min as the BA-SHA interaction rapidly re-established (Fig. 4B). However, further recovery was slow as the diffusion of the cross-links in a dynamic covalent system is generally limited by the rate of boronic acid-SHA scrambling. Nonetheless, the system remains robust under repetitive stress cycles (Fig. S31). Longer PEG chains showed better recovery because higher water content within the system facilitates diffusion and thus re-establishment of the intermolecular bonds. In contrast, branched PEG chains like the 4-arm PEG_{2000}-$(SHA)_2$ do not show rapid self-healing properties as they are much more rigid and compact thus making them more difficult to bridge the protein molecules.

As these intermolecular bonds often require energy to exchange more efficiently, we postulate that by increasing the temperature of the system, healing would be more efficient. By raising the temperature from 25 °C to 37 °C, although the G′/G″ parameters increase by ~25% (Fig. 4C), the modulus crossover decreased from 437% to 324% as the matrix weakens (Fig. 4D). However, the self-healing properties remain largely similar which may suggest that the increase in diffusion speed alone cannot compensate the loss in binding energy between the interacting groups. Nonetheless, for

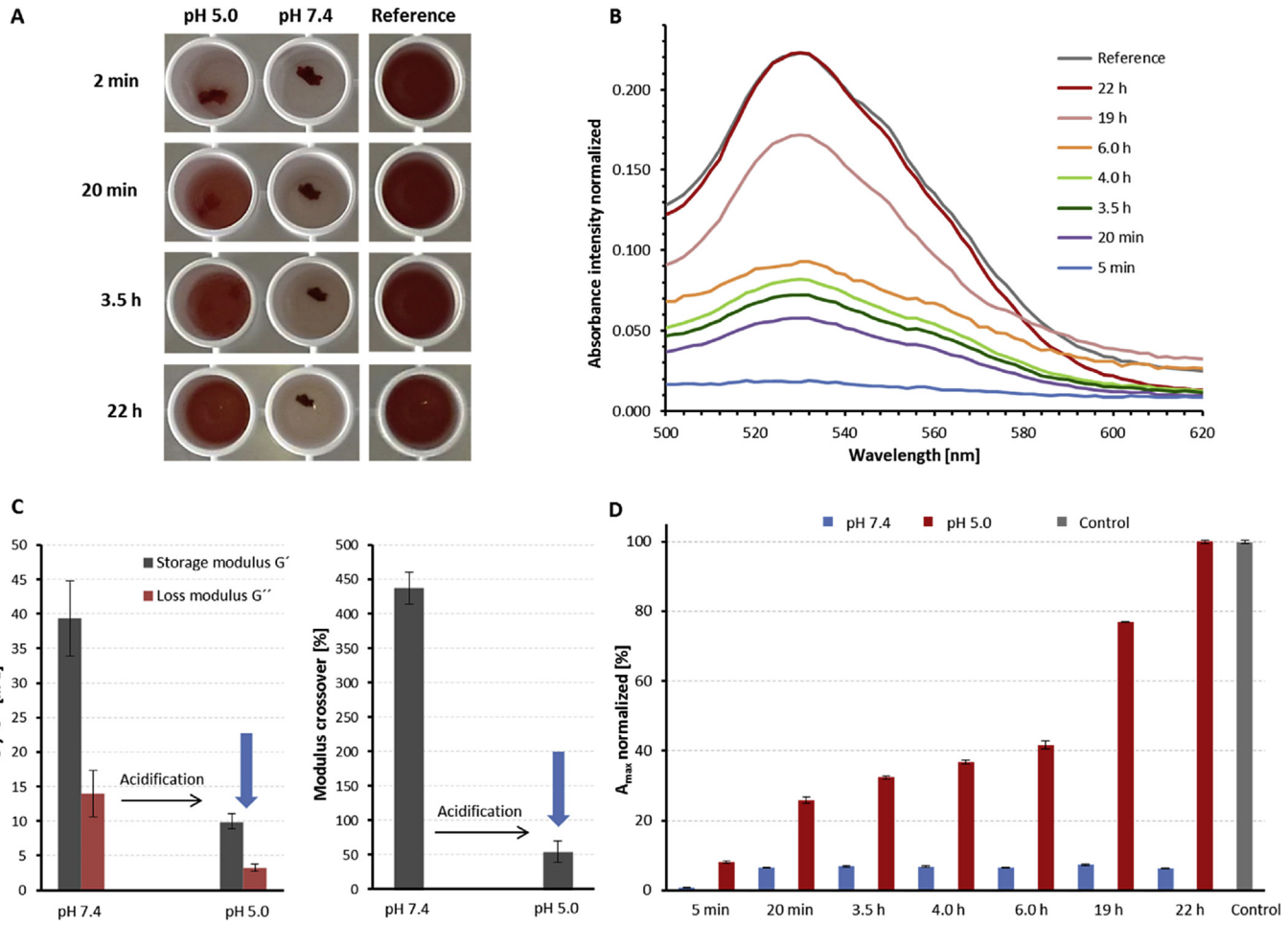

Fig. 3. Hydrogel responsiveness to pH. A) Time lapsed optical images of the CytC hydrogel incubated in pH 5.0 and pH 7.4 buffer. Reference contains the equivalent amount of CytC in solution. B) Absorbance spectra of the supernatant containing CytC hydrogel in pH 5.0 buffer at different time intervals. Reference spectrum denotes 100% release of protein. C) Change in storage and loss modulus (left) as well as decrease in modulus crossover (right) as a response to acidification to pH 5.0. D) Protein release kinetics at pH 5.0 (red) and at pH 7.4 (blue). Absorbance is normalized to CytC-BA in solution. All data presented as ±SEM, n = 3.

the linear cross-links, even with multiple cycles of healing, the general mechanical properties of the gel remain largely intact.

2.4. Biological functions and cellular applications

With these aforementioned mechanical properties, we show that even sensitive enzymes can be incorporated into robust and responsive hybrid materials by chemical design. We next seek to establish a biological function and demonstrate that the material retains the catalytic properties of the enzyme in its native form.

CytC is an enzyme that exhibits peroxidase activity due to the Fe^{3+} ion within the heme group at its core. A colorimetric assay based on 2,2′-azino-bis(3-ethylbenzothiazoline-6-sulphonic acid) (ABTS) was used to analyze the enzyme kinetics of the CytC-BA within the hydrogel. The assay was conducted using a hydrogel containing CytC-BA (85 μM) as well as with a solution of CytC-BA (85 μM) as a reference (Fig. 5A). The absorbance was monitored at 410 nm and the results showed that the protein activity was quantitatively conserved as both the solution and hydrogel CytC-BA reaches the same absorbance maximum. Naturally, the rate of which the enzyme exhibits its maximum activity is slower in the hydrogel system because it is limited by diffusion of ABTS into the gel matrix (Fig. 5B). However, the peroxidase activity of CytC is only dependent on the Fe^{3+} active center and not the enzyme as a whole. CytC initiates apoptosis in cells by self-assembling into a heptameric assembly called the apoptosome which cleaves the caspases 2, 8, 9 and 10 to initiate the apoptotic cascade. In this aspect, the structural integrity of the enzyme is crucial for the apoptosome assembly. Hence, the hydrogel was introduced into A549 human alveolar adenocarcinoma cells and its resultant apoptosis effect was quantified using CellTiter-Glo® cell viability assay. The hydrogel was first constructed under sterile conditions on a glass microscope slide and transferred into a 24-well cell culture plate containing A549 cells. As a reference, the same amount of CytC-BA (23 and 57 μM) used in the hydrogel was introduced as a solution into a separate well. Additional as controls, the PEG_{2000}-$(SHA)_2$ cross linker (630 μM) and doxorubicin (20 μM) were used. The cells were incubated for 24 h to analyze and compare the protein activity and release. Significant apoptosis (>45%) of A549 cells can be detected upon administration of the hydrogel at 57 μM which is similar as the free CytC-BA (Fig. 5C). In comparison to the positive control, the hydrogel exhibits a similar potency to doxorubicin (20 μM) which is a widely used chemo-therapeutic against cancer. The induced apoptosis was attributed to the intracellular CytC activity as the PEG_{2000}-$(SHA)_2$ (630 μM) did not show apparent toxicity towards A549 cells.

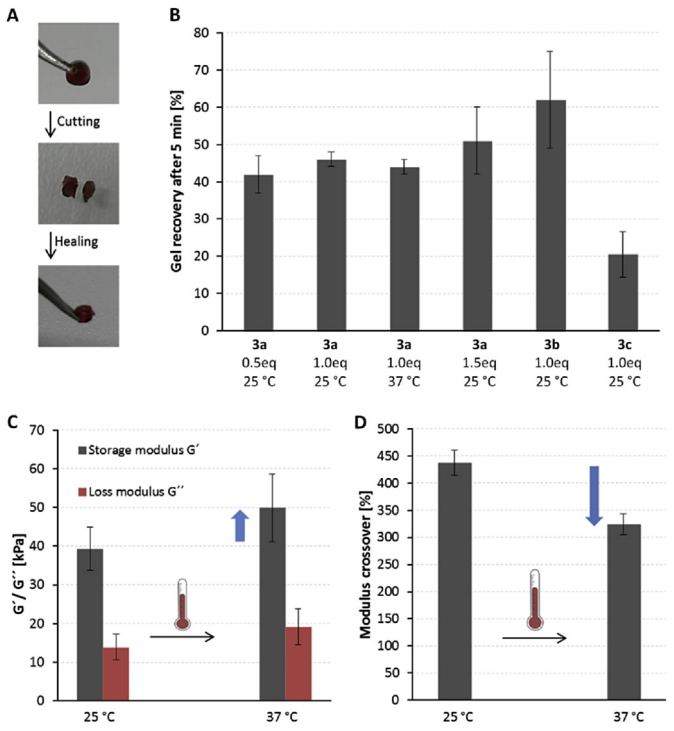

Fig. 4. Self-healing and temperature dependency of CytC-BA hydrogel. A) Optical images of gel reattachment. B) Quantification of gel recovery after 5 min of relaxation for each cross-linker analogue. C) Increase in viscoelastic parameters G′ and G″ as temperature increases from 25 °C to 37 °C. D) Decrease in gel stability with increase in temperature.

3. Conclusion

In summary, we have created a smart hydrogel system based on a native enzyme acting both as a structural and bioactive component. As such, the dynamic covalent chemistry based on boronic acid/salicyl hydroxamate enables bioorthogonal crosslinking technology that is responsive under mild aqueous conditions to preserve the functions of the enzyme.

Although the hydrogel comprises conformationally sensitive protein molecules, the resultant mechanical strength in terms of storage and loss modulus is very high in comparison to other dynamic or supramolecular systems. In addition, these gels show self-healing and pH dependent behavior that is representative of the dynamism of the cross-linker chemistry. The proteins can be effectively released in a physiological environment and exert their original apoptosis activity within cancer cells. Thus, we have created here a minimalistic hydrogel platform where sensitive macromolecules can be responsively cross-linked in a facile manner. In perspective, by streamlining the chemical technology, multicomponent hydrogels consisting of different interacting biomolecules can be incorporated to increase complexity and material "intelligence" such as cascading triggers and feedback mechanisms.

4. Experimental section

4.1. Synthesis

All solvents and reagents are bought from commercial sources (Merck, Sigma Aldrich, VWR, etc.) and are used directly without further purification. The amine functionalized PEGs were purchased from Rapp Polymers. For column chromatography silica gel 60 M (0.040–0.063 mm) from Macherey-Nagel was used. Cytochrome c from equine heart was ordered from Sigma Aldrich in ≥95% purity (SDS-Page). All other chemicals/biologicals including e.g. DMEM cell culture medium are purchased from multiple commercial sources (Merck, Alfa Aesar, Invitrogen etc.) and used directly without further purification. ^{1}H NMR spectra are recorded using Bruker AVANCE III 300 using deuterated solvents as mentioned. Chemical shifts are reported as parts per million referenced with respect to the residual solvent peak. FT-IR spectra were recorded using a Thermo Scientific iS10FT-IR spectrometer, equipped with a diamond ATR unit. MALDI TOF MS was performed on Bruker Daltonics Reflex III. Absorbance measurements are taken from Tecan 20 M spark microplate reader, luminescence readings were accomplished by using a Tecan Infinite M1000 microplate reader. All rheological experiments were performed using the Discovery Hybrid Rheometer 3 from TA Instruments, equipped with an 8 mm flat geometry including a solvent reservoir and suitable cap/rings to create a closed chamber. A Peltier Plate, which allows temperature control, was used as well as Trios as related software for sample processing. Purification of Trt-protected SHA-PEGs was realized using a recycling GPC system from Shimadzu using SEC columns from JAIGEL (JAIGEL-1H and -2H columns in a row). Protein modification solutions were purified via ultrafiltration using Vivaspin 20 (MWCO 5000) tubes from Sartorius. The

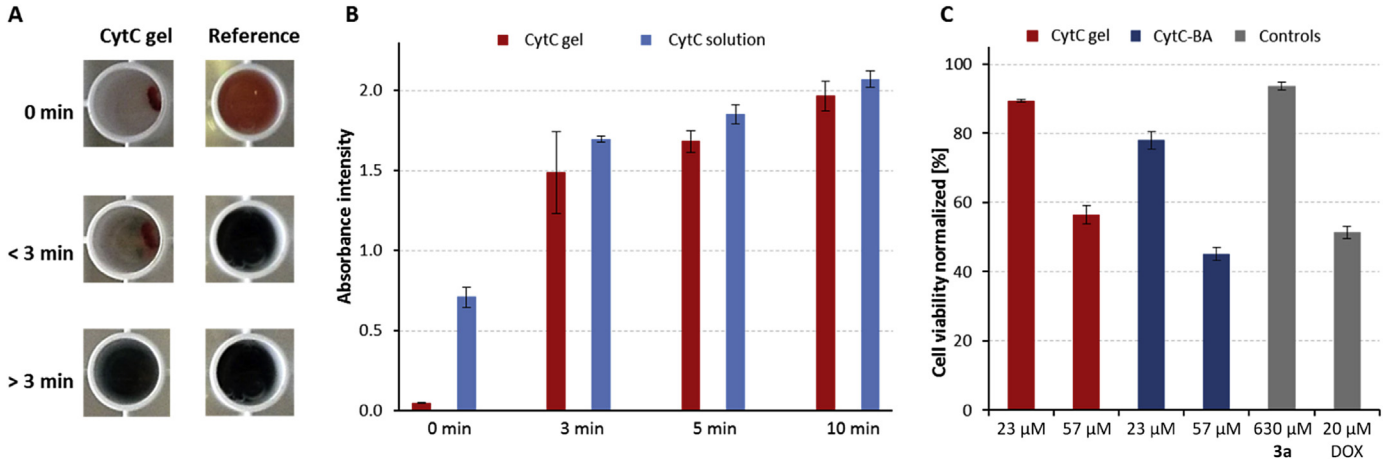

Fig. 5. Peroxidase activity and apoptosis induction of cytochrome c hydrogel. A) Colorimetric assay of cytochrome c hydrogel (85 µM) using ABTS assay. B) Quantification of peroxidase activity on ABTS by absorbance spectroscopy. C) Cell viability assay on the capability of cytochrome c to induce apoptosis in A549 cells. Data represented as ±SEM, n = 3.

grade of water (H_2O) used is MilliQ ultrapure grade.

*4.1.1. Synthesis of PEG$_x$-(N$_3$)$_y$ (**1a**, **1b**, **1c**)*

Amine-functionalized PEGs (PEG_{2000}-$(NH_2)_2$, PEG_{3000}-$(NH_2)_2$, 4-arm PEG_{2000}-$(NH2)_4$) were purchased from Rapp Polymers. The following synthesis procedure is given for PEG_{2000}-$(NH_2)_2$ conversion. The PEG (0.30 g, 0.15 mmol) was dissolved in 20 mL water. Copper sulfate (0.12 eq, 3.00 mg, 0.02 mmol) and potassium carbonate (7.00 eq, 0.15 g, 1.05 mmol) were added to the reaction solution. Imidazol-1-sulfonyl azide hydrochloride was synthesized as reported in literature and used as an azido transfer reagent to convert the amine compound into its azide derivative. Addition of imidazol-1-sulfonyl azide hydrochloride (i, 2.60 eq, 0.08 g, 0.39 mmol) to reaction solution was performed and stirred at room temperature overnight. The next day, hydrochloric acid (1 M, 30 mL) was added to acidify the reaction solution. The azide-functionalized PEG was extracted with dichloromethane (x5) and the collected organic layers were dried with sodium sulfate. After removal of solvent and drying under vacuum, the product 1a was obtained as transparent oil in 96% yield (0.295 g, 0.14 mmol).

PEG_{2000}-$(N_3)_2$ (**1a**): ^{1}H NMR (300 MHz, CD_2Cl_2) δ [ppm] = 3.83 (t, 4H, $C\underline{H}_2$–N_3), 3.60 (m, O–$C\underline{H}_2C\underline{H}_2$), 3.38 (m, 12H, $(C\underline{H}_2)_n$-CH_2–N_3). FT-IR ν [cm^{-1}] = 2879, 2104, 1469, 1341, 1281, 1238, 1143, 1100, 1060, 954, 842, 526.

PEG_{3000}-$(N_3)_2$ (**1b**): ^{1}H NMR (300 MHz, CD_2Cl_2) δ [ppm] = 3.83 (t, 4H, $C\underline{H}_2$–N_3), 3.60 (m, O–$C\underline{H}_2C\underline{H}_2$), 3.38 (m, 12H, $(C\underline{H}_2)_n$-CH_2–N_3). FT-IR ν [cm^{-1}] = 2877, 2102, 1464, 1341, 1278, 1233, 1148, 1095, 1060, 960, 842, 529.

4-arm PEG_{2000}-$(N_3)_4$ (**1c**): ^{1}H NMR (300 MHz, CD_2Cl_2) δ [ppm] = 3.83 (t, 4H, HC$\underline{H}$–N_3), 3.60 (m, O–$C\underline{H}_2C\underline{H}_2$), 3.41 (m, 24H, $(C\underline{H}_2)_n$-$\underline{H}$CH–N_3). FT-IR ν [cm^{-1}] = 2674, 2384, 2350, 2328, 2111, 1334, 978.

4.1.2. Synthesis of protected PEG$_x$-(SHA-Trt)$_y$

The following synthesis procedure is given representative for PEG_{2000}-$(N_3)_2$ (**1a**) conversion into the Trt-protected SHA-PEG (**2a**) as it was performed comparably for the other PEG derivatives. The azide-functionalized PEG (**1a**, 0.19 g, 0.09 mmol) was dissolved in tetrahydrofurane (4 mL). Ethynyl salicyl hydroxamic acid (**ii**, 2.20 eq, 0.10 g, 0.20 mmol, synthesized as reported previously within our group[17]) was added to the reaction solution. Copper sulfate (2.60 eq, 0.04 g, 0.24 mmol) and sodium ascorbate (2.80 eq, 0.05 g, 0.26 mmol) were dissolved in water (4 mL) and added to the reaction mixture. The copper-catalyzed azide-alkyne cycloaddition was performed stirring overnight at room temperature. After purification of the raw product by silica gel column chromatography (eluent: dichloromethane/methanol − 9/1 to 8/2), the solvent was removed. For further purification using a recycling GPC system (SEC columns: JAIGEL 1H and 2H in a row), the intermediate was redissolved in chloroform. The product **2a** was obtained after separation and drying under vacuum yielding as brownish oil in 60% (0.17 g, 0.06 mmol).

PEG_{2000}-(SHA-Trt)$_2$ (**2a**): ^{1}H NMR (300 MHz, CD_2Cl_2) δ [ppm] = 11.18 (s, 2H, Ph-O$\underline{H}$), 8.71 (s, 2H, N$\underline{H}$-Ph), 8.45 (s, 2H, CO–N$\underline{H}$–O), 7.60 (s, 2H, N–C$\underline{H}$=C–N), 7.50 (dd, 12H, *m*-H_{Ar} of TrtO), 7.33 (m, 18H, *o*-H_{Ar} of TrtO, *p*-H_{Ar} of TrtO), 7.15 (d, 2H, H_{Ar}), 7.00 (m, 4H, H_{Ar}), 4.46 (t, 4H, $C\underline{H}_2$–N), 3.78 (t, 4H, C$\underline{H}$2–O), 3.59 (m, $C\underline{H}_2C\underline{H}_2$–O), 3.05 (t, 4H, $C\underline{H}_2$–CH_2–CO–NH), 2.74 (t, 4H, CH_2–$C\underline{H}_2$–CO–NH).

PEG_{3000}-(SHA-Trt)$_2$ (**2b**): ^{1}H NMR (300 MHz, CD_2Cl_2) δ [ppm] = 11.17 (s, 2H, Ph-O$\underline{H}$), 8.68 (s, 2H, N$\underline{H}$-Ph), 8.39 (s, 2H, CO–N$\underline{H}$–O), 7.60 (s, 2H, N–C$\underline{H}$=C–N), 7.49 (dd, 12H, *m*-H_{Ar} of TrtO), 7.34 (m, 18H, *o*-H_{Ar} of TrtO, *p*-H_{Ar} of TrtO), 7.15 (d, 2H, H_{Ar}), 7.01 (m, 4H, H_{Ar}), 4.47 (t, 4H, $C\underline{H}_2$–N), 3.78 (t, 4H, C$\underline{H}$2–O), 3.60 (m, $C\underline{H}_2C\underline{H}_2$–O), 3.05 (t, 4H, $C\underline{H}_2$–CH_2–CO–NH), 2.74 (t, 4H, CH_2–$C\underline{H}_2$–CO–NH).

4-arm PEG_{2000}-(SHA-Trt)$_4$ (**2c**): ^{1}H NMR (300 MHz, CD_2Cl_2) δ [ppm] = 11.21 (s, 4H, Ph-O$\underline{H}$), 9.49 (s, 4H, N$\underline{H}$-Ph), 8.85 (s, 4H, CO–N$\underline{H}$–O), 7.61 (s, 4H, N–C$\underline{H}$=C–N), 7.51 (dd, 24H, *m*-H_{Ar} of TrtO), 7.32 (m, 40H, *o*-H_{Ar} of TrtO, *p*-H_{Ar} of TrtO, H_{Ar}), 7.18 (d, 4H, H_{Ar}), 6.99 (m, 4H, H_{Ar}), 4.45 (t, 8H, $C\underline{H}_2$–N), 3.77 (t, 8H, C$\underline{H}$2–O), 3.56 (m, $C\underline{H}_2C\underline{H}_2$–O), 3.04 (t, 8H, $C\underline{H}_2$–CH_2–CO–NH), 2.73 (t, 8H, CH_2–$C\underline{H}_2$–CO–NH).

4.1.3. Synthesis of PEG$_x$-(SHA)$_y$ cross-linkers

The following synthesis procedure is given representative for Trt-protected PEG_{2000}-$(SHA)_2$ (**2a**) conversion into the PEG_{2000}-$(SHA)_2$ (**3a**) as it was performed comparably for the other PEG derivatives. The Trt-protected SHA-functionalized PEG (**2a**, 0.11 g, 0.04 mmol) was dissolved in dichloromethane (4.0 mL). Triisopropylsilane (2.0 mL, 21% *v/v*) and trifluoroacetic acid (TFA, 3.5 mL, 37% *v/v*) were added dropwise to the reaction solution. After 3 h stirring at room temperature the solvent and TFA were evaporated under vacuum. Water was added to the solid and the aqueous phase was washed with toluene. The cross-linker **3a** was obtained by lyophilisation of the aqueous phase as brownish oil in 98% yield (0.09 g, 0.04 mmol).

PEG_{2000}-$(SHA)_2$ (**3a**): ^{1}H NMR (300 MHz, CD_2Cl_2) δ [ppm] = 8.98 (s, 2H, N$\underline{H}$-Ph), 7.99 (s, 2H, N–C$\underline{H}$=C–N), 7.53 (m, 2H, H_{Ar}), 7.34 (m, 2H, H_{Ar}), 7.02 (m, 2H, H_{Ar}), 4.58 (t, 4H, $C\underline{H}_2$–N), 3.84 (t, 4H, C$\underline{H}$2–O), 3.61 (m, $C\underline{H}_2C\underline{H}_2$–O), 3.21 (t, 4H, $C\underline{H}_2$–CH_2–CO–NH), 2.84 (t, 4H, CH_2–$C\underline{H}_2$–CO–NH). GPC (DMF) D = 1.47.

PEG_{3000}-$(SHA)_2$ (**3b**): ^{1}H NMR (300 MHz, CD_2Cl_2) δ [ppm] = ^{1}H NMR (300 MHz, CD_2Cl_2) δ [ppm] = 8.92 (s, 2H, N$\underline{H}$-Ph), 7.94 (s, 2H, N–C$\underline{H}$=C–N), 7.52 (m, 2H, H_{Ar}), 7.32 (m, 2H, H_{Ar}), 7.08 (m, 2H, H_{Ar}), 4.57 (t, 4H, $C\underline{H}_2$–N), 3.84 (t, 4H, C$\underline{H}$2–O), 3.61 (m, $C\underline{H}_2C\underline{H}_2$–O), 3.20 (t, 4H, $C\underline{H}_2$–CH_2–CO–NH), 2.84 (t, 4H, CH_2–$C\underline{H}_2$–CO–NH). GPC (DMF) D = 1.70.

4-arm PEG_{2000}-$(SHA)_4$ (**3c**): ^{1}H NMR (300 MHz, CD_2Cl_2) δ [ppm] = 9.11 (s, 4H, N$\underline{H}$-Ph), 7.56 (s, 4H, N–C$\underline{H}$=C–N), 7.27 (m, 4H, H_{Ar}), 7.13 (d, 4H, H_{Ar}), 7.11 (m, 4H, H_{Ar}), 4.54 (t, 8H, $C\underline{H}_2$–N), 4.18 (t, 8H, C$\underline{H}$2–O), 3.59 (m, $C\underline{H}_2C\underline{H}_2$–O), 3.04 (t, 8H, $C\underline{H}_2$–CH_2–CO–NH), 2.73 (t, 8H, CH_2–$C\underline{H}_2$–CO–NH). GPC (DMF) D = 1.47.

4.1.4. Synthesis of CytC-BA

Cytochrome c (200.0 mg, 0.016 mmol) from equine heart was dissolved in phosphate buffer (pH 8.0, 50 mM, 20 mL) and was shaken at 350 rpm at room temperature. 4-Carboxyphenylboronic acid succinimidyl ester (synthesized as reported previously,[18] 18 eq, 76.5 mg, 0.291 mmol) was dissolved in dimethyl sulfoxide (400 μL) and added to the protein solution. Reaction was further shaken overnight. Purification was carried out by ultrafiltration using Vivaspin 20 (molecular weight cut off 5000 Da) tubes at 3800 rpm and 4 °C. After removal of buffer solution, the protein was washed with MilliQ ultrapure water four times. The modified CytC was obtained in 96% yield as red powder by lyophilisation. Analysis was done by MALDI TOF MS (matrix: sinapinic acid) and resulted in 11 boronic acid groups as protein functionalization (calculation was performed related to the MS of the native CytC, see Supplementary Fig. S1).

4.1.5. Synthesis of CytC-BA hydrogels

The boronic acid-modified cytochrome c (CytC-BA) was dissolved in phosphate buffer (pH 7.4, 100 mM) as a stock solution (160 mg/mL). The respective cross-linker was dissolved in phosphate buffer (pH 7.4, 100 mM, eq. in relation to SHA-moiety per BA binding event). Hydrogels were obtained by mixing CytC-BA solution and cross-linker solution 1: 1 (volume related to desired gel size). Mixing of both solutions by an Eppendorf pipette needs to be

done with special care and adjusted speed as the gel formation starts instantaneously. Characterization of the obtained CytC gels (8 wt %) was performed by rheological characterization as described in the following section.

4.2. Rheology

All rheological experiments were performed using the Discovery Hybrid Rheometer 3 (DHR3) from TA instruments. Temperature was always controlled by a Peltier plate. All samples were measured using an 8 mm flat geometry (stainless steel), which is equipped with a solvent reservoir (filled with water). To prevent drying of hydrogel samples during measurement, a closing ring/cap system was attached to the geometry additionally to the solvent trap to create a closed chamber. The gels were always created on the measuring plate (30 μL gels, 8 wt %) and gelation kinetics were monitored directly. If not specified differently, all samples were performed at 25 °C and with 0.25 mm mess gap. They were tracked by their gelation until they reach a steady state, to carry out the desired experiment then (e.g. amplitude sweep). All experiments were performed in triplicates.

4.2.1. Kinetics measurements

Gelation kinetics was always monitored before performing any other experiment. Therefore, the CytC gels were studied for 1 h under fixed 1.0% oscillatory strain and 1.0 Hz frequency. Reaching a steady state for G′/G″ of a gel sample, a 5 min time sweep (1.0% strain, 1.0 Hz frequency) was always carried out to show the equilibrated material behavior. Other rheological measurements were conducted subsequently.

4.2.2. Oscillatory strain

The amplitude sweep was done to characterize the gel matrix stability/stiffness towards mechanical stress. By applying 0.01% up to 1000% oscillatory strain at fixed 1.0 Hz frequency to a hydrogel, the network breaks down at a certain point. Defined as modulus crossover point because of increase of loss modulus G″ over storage modulus G′, this point highlights where the gel assumes an elastic fluid behavior.

4.2.3. Gel recovery (self-healing)

After performance of an amplitude sweep resulting in total network destruction of the hydrogel, it was allowed to self-heal by removing mechanical stress. To track the network re-formation by increasing G′/G″ values, 0.1% strain at 1.0 Hz frequency were chosen as conditions. The storage and loss modulus obtained after 5 min of gel healing were related to starting values of G′/G″ (100% were set for G′/G″ before network destruction).

4.2.4. Temperature effects

For screening temperature effects on CytC gels at 37 °C (physiological temperature), the hydrogels were built under 25 °C and monitored in their gelation. After reaching steady state, they were warmed up with 1 °C per minute controlled by the Peltier element of the rheometer (tracking G′/G″ under fixed strain 1.0% and frequency 1.0 Hz). After temperature elevation from 25 °C to 37 °C and time sweep (37 °C, 5 min, 1.0% strain, 1.0 Hz frequency), the hydrogels were characterized by amplitude sweep as well as gel recovery at 37 °C.

4.2.5. pH responsiveness

CytC gels were formed as for all other rheological experiments (components are dissolved in phosphate buffer pH 7.4). After addition of hydrogen chloride solution (0.5 M) onto CytC gel to acidify to pH 5, the network kinetics/gel dissolution was monitored by performing directly a time sweep experiment (1.0% strain, 1.0 Hz frequency, 1 h). Decrease of storage and loss modulus of hydrogel due to shifting the equilibrium of PBA-SHA interaction towards decomplexation seems to reach a steady state after ~ 1 h. Amplitude sweep of gel under pH 5 was performed with 1.0 Hz frequency and 0.01–1000% strain.

4.3. Biological experiments

4.3.1. Protein release as a function of pH

The experiment was performed using a 96-well white, chimney well microplate (Cellstar®). CytC gels (5 μL gels, 8 wt %) were prepared on a microscope glass slide using **3a** (1.0 eq SHA moiety per BA) and was transferred thereafter into the solutions. Phosphate buffer pH 7.4 and pH 5.0 (100 mM, 200 μL) were already filled into each well. As reference to the protein hydrogels, CytC-BA solutions were added to the wells to have equal CytC concentration within each well (either dissolved or within the gel). Optical images as well as absorbance scans (500–620 nm, 530 nm values were taken for protein release kinetic study) were carried out. At each time point, 20 μL of the supernatant/solution of each well was transferred into wells of a 384 transparent, flat bottom microplate (UV-Star®) for scanning and afterwards all solutions were transferred back into the original well, from where they were taken out. Various time intervals were chosen for optical images of the samples and measuring their absorbance intensity related to dissolved/released CytC within the buffer solution (5 min, 20 min, 3.5 h, 4.0 h, 6.0 h, 19 h and 22 h). All samples were performed in triplicates.

4.3.2. Enzyme activity assay

Experiment was performed using a 96 white, chimney well microplate (Cellstar®). CytC gels (3 μL gels, 8 wt %) were prepared on a microscope glass slide using 3a (1.0 eq SHA moiety per BA) and afterwards transferred into the solutions. Phosphate buffer pH 7.4 (100 mM, 166 μL) as well as ABTS solution (10 mM, 20 μL) were already filled into each well. As reference to the protein hydrogels CytC-BA solutions (85 μM well concentration) were added to the wells. First measurement was performed before addition of hydrogen peroxide solution. Therefore 20 μL of the supernatant/solution of each well was transferred into wells of a 384 transparent, flat bottom microplate (UV-Star®) for scanning and afterwards all solutions were transferred back into the original well, from where they were taken out. This was repeated for each scanning step. For starting the enzyme activity assay, hydrogen peroxide solution (0.1 M, 3 μL) was added to each well. Optical images as well as absorbance measurements at 410 nm were performed in different time intervals (absorbance scans at 0 min and after 3 min, 5 min and 10 min). All samples were carried out in triplicates.

4.3.3. Cell culture

Cell culture of A549 cells was performed in Dulbecco's Modified Eagle's Medium (DMEM, High Glucose) supplemented with 10% FBS, 1% penicillin/streptomycin and 1x MEM non-essential amino acid with incubation conditions set at 37 °C, 5% CO_2. CellTiter-Glo® Cell Viability Assay was purchased from Promega and used according to the given protocol.

4.3.4. Cytotoxicity assay

A549 cells were seeded at a density of 15,000 cells per well in a 24-well culture plate and allowed to adhere overnight at 37 °C, 5% CO_2. Hydrogels (1 μL, 5 μL sized gels, 8 wt%) were prepared separately on top of a sterile microscope slide by mixing a solution of PEG_{2000}-$(SHA)_2$ (1.0 eq. per BA motif) with CytC-BA at the prescribed final concentration (23 μM, 57 μM). The hydrogels were

subsequently transferred cleanly into each well in triplicates and allowed to incubate for 24 h at 37 °C, 5% CO_2. Controls consisting of solution CytC-BA, PEG_{2000}-$(SHA)_2$ (**3a,** 630 μM) and doxorubicin (DOX, 20 μM) were introduced into separate wells in triplicates. After incubation, the cells were treated with CellTiter-Glo® luminescence cell viability assay according to manufacturer's protocol and scanned using Tecan M1000 Infinite microplate reader.

Acknowledgments

We are grateful to the financial support from the Horizon2020 project ADGUT (ID: 686271) as well as the Volkswagenstiftung (Project ID: 86366).

Appendix A. Supplementary data

Supplementary data related to this article can be found at http://dx.doi.org/10.1016/j.tet.2017.06.066.

References

1. Mattia E, Otto S. Supramolecular systems chemistry. *Nat Nanotechnol*. 2015;10(2):111–119.
2. Webber MJ, Appel EA, Meijer EW, Langer R. Supramolecular biomaterials. *Nat Mater*. 2016;15(1):13–26.
3. Zhao D, van Leeuwen T, Cheng J, Feringa BL. Dynamic control of chirality and self-assembly of double-stranded helicates with light. *Nat Chem*. 2017;9(3):250–256.
4. Lehn J-M. Toward complex matter: supramolecular chemistry and self-organization. *Proc Natl Acad Sci U. S. A*. 2002;99(8):4763–4768.
5. Grzybowski BA, Huck WTS. The nanotechnology of life-inspired systems. *Nat Nanotechnol*. 2016;11(7):585–592.
6. Sevier CS, Kaiser CA. Formation and transfer of disulphide bonds in living cells. *Nat Rev Mol Cell Biol*. 2002;3(11):836–847.
7. Góngora-Benítez M, Tulla-Puche J, Albericio F. Multifaceted roles of disulfide bonds. Peptides as therapeutics. *Chem Rev*. 2014;114(2):901–926.
8. Gruber CW, Čemažar M, Heras B, Martin JL, Craik DJ. Protein disulfide isomerase: the structure of oxidative folding. *Trends Biochem Sci*. 2006;31(8):455–464.
9. Hogg PJ. Targeting allosteric disulphide bonds in cancer. *Nat Rev Cancer*. 2013;13(6):425–431.
10. Mulvey M, Brown DT. Formation and rearrangement of disulfide bonds during maturation of the Sindbis virus E1 glycoprotein. *J Virol*. 1994;68(2):805–812.
11. Xu S, Sankar S, Neamati N. Protein disulfide isomerase: a promising target for cancer therapy. *Drug Discov Today*. 2014;19(3):222–240.
12. Stolowitz ML, Ahlem C, Hughes KA, et al. Phenylboronic Acid–Salicylhydroxamic acid bioconjugates. 1. A novel boronic acid complex for protein immobilization. *Bioconjug Chem*. 2001;12(2):229–239.
13. Bull SD, Davidson MG, van den Elsen JMH, et al. Exploiting the reversible covalent bonding of boronic acids: recognition, sensing, and assembly. *Acc Chem Res*. 2013;46(2):312–326.
14. Martínez-Aguirre MA, Villamil-Ramos R, Guerrero-Alvarez JA, Yatsimirsky AK. Substituent effects and pH profiles for stability constants of arylboronic acid diol esters. *J Org Chem*. 2013;78(10):4674–4684.
15. Arzt M, Seidler C, Ng DYW, Weil T. Reversible click reactions with boronic acids to build supramolecular architectures in water. *Chem Asian J*. 2014;9(8):1994–2003.
16. Shin SBY, Almeida RD, Gerona-Navarro G, Bracken C, Jaffrey SR. Assembling ligands in situ using bioorthogonal boronate ester synthesis. *Chem Biol*. 2010;17(11):1171–1176.
17. Ng DYW, Arzt M, Wu Y, Kuan SL, Lamla M, Weil T. Constructing hybrid protein zymogens through protective dendritic assembly. *Angew Chem Int Ed*. 2014;53(1):324–328.
18. Seidler C, Ng DYW, Wu Y, Weil T. pH responsive supramolecular core-shell protein hybrids. *Supramol Chem*. 2016;28(9-10):742–746.
19. Olsen BD, Kornfield JA, Tirrell DA. Yielding behavior in injectable hydrogels from telechelic proteins. *Macromolecules*. 2010;43(21):9094–9099.
20. Zehner NA, Dietrick SM, Tirrell DA, Kennedy SB. Two-site internally cooperative mechanism for enzyme kinetics in a hydrogel forming recombinant protein. *Biomacromolecules*. 2015;16(11):3651–3656.
21. Bastings MMC, de Greef TFA, van Dongen JLJ, Merkx M, Meijer EW. Macrocyclization of enzyme-based supramolecular polymers. *Chem Sci*. 2010;1(1):79–88.
22. Oliva N, Conde J, Wang K, Artzi N. Designing hydrogels for on-demand therapy. *Acc Chem Res*. 2017;50(4):669–679.
23. Xu J, Strandman S, Zhu JXX, Barralet J, Cerruti M. Genipin-crosslinked catechol-chitosan mucoadhesive hydrogels for buccal drug delivery. *Biomaterials*. 2015;37:395–404.
24. Choh S-Y, Cross D, Wang C. Facile synthesis and characterization of disulfide-cross-linked hyaluronic acid hydrogels for protein delivery and cell encapsulation. *Biomacromolecules*. 2011;12(4):1126–1136.
25. Pan W, Wen H, Niu L, et al. Effects of chain flexibility on the properties of DNA hydrogels. *Soft Matter*. 2016;12(25):5537–5541.
26. Ren C, Song Z, Zheng W, et al. Disulfide bond as a cleavable linker for molecular self-assembly and hydrogelation. *Chem Commun*. 2011;47(5):1619–1621.
27. Lee JH, Park J, Park J-W, Ahn H-J, Jaworski J, Jung JH. Supramolecular gels with high strength by tuning of calix[4]arene-derived networks. *Nat Commun*. 2015;6:6650.
28. Rowland MJ, Atgie M, Hoogland D, Scherman OA. Preparation and supramolecular recognition of multivalent peptide–polysaccharide conjugates by Cucurbit[8]uril in hydrogel formation. *Biomacromolecules*. 2015;16(8):2436–2443.
29. Chen H, Hou S, Ma H, Li X, Tan Y. Controlled gelation kinetics of cucurbit[7]uril-adamantane cross-linked supramolecular hydrogels with competing guest molecules. *Sci Rep*. 2016;6:20722.
30. Bastings MMC, Koudstaal S, Kieltyka RE, et al. A fast pH-switchable and self-healing supramolecular hydrogel carrier for guided, local catheter injection in the infarcted myocardium. *Adv Healthc Mater*. 2014;3(1):70–78.